Time-Domain Synthesis of Conical Bore Instrument Sounds

Gary P. Scavone
gary@ccrma.stanford.edu

Center for Computer Research in Music and Acoustics
Department of Music, Stanford University
Stanford, California 94305-8180 USA

Abstract

This paper presents a series of approaches for discrete time-domain synthesis of conical bore instrument sounds. The generation of steady, self-sustained oscillations using conical waveguides is complicated by properties inherent to truncated conic frusta. Two different physical structures are discussed which can be characterized by the same circuit diagram. A more abstract and flexible "virtual" model is presented which is capable of synthesizing half-wave resonators with a rich variety of timbres. Implementations using digital waveguide techniques are described.

1 Introduction

Active research in time-domain synthesis of wind instrument sounds has continued for over two decades. Many instruments, such as clarinets, flutes, and trumpets, have been synthesized using time-domain models with very good sonic results [Cook 1992, Verge 1995, Vergez and Rodet 1998]. Successful, robust models of conical bore instruments, however, have been more difficult to achieve. This paper explores the acoustic properties of conic frusta and the resulting impediments to robust synthesis of conical bore sounds. With an emphasis on model simplicity and efficiency, several different approaches are presented.

2 Synthesis Methods

This study makes use of digital waveguide synthesis techniques to model the air column of a conical bore instrument [Smith 1992]. Digital waveguides efficiently implement ideal, lossless, and linear traveling-wave propagation using digital delay lines, as depicted in Fig. 1. Linear losses can be commuted and implemented at discrete locations within the system.

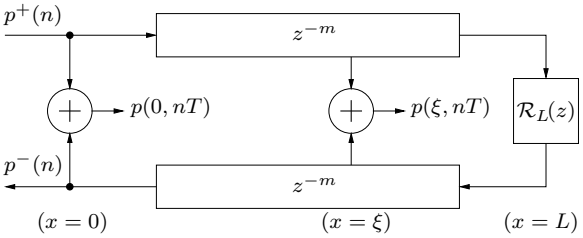

Figure 1: Digital waveguide implementation of plane-wave propagation in a cylindrical pipe, neglecting viscothermal losses.

The primary concern in this paper is the use of a conic frustum model in the synthesis of wind instrument sounds. Despite the asymmetries exhibited by real conical wind instrument bodies, we assume that a single conic section will adequately approximate the majority of the modeled air column.

A simple memory-less, non-linear reed function is used for the realtime implementations discussed here. The reed-channel volume flow and pressure difference characteristic, shown in Fig. 2, is solved in terms of a non-linear traveling-wave reflection function [Smith 1986] as:

$$p_o^+ = r(p_\Delta)\left[p_o^- - \frac{p_b}{2}\right] + \frac{p_b}{2},$$

where

$$r(p_\Delta) = \frac{Z_r(p_\Delta) - Z_o}{Z_r(p_\Delta) + Z_o},$$

p_o is the pressure at the air column input, p_b is the player's breath pressure, $p_\Delta = p_b - p_o$ is the pressure difference across the reed, Z_r is a time-varying reed "impedance", and Z_o is the real wave impedance at the air column input.

Good results have been achieved using the simplified reed reflection function shown at the bottom of Fig. 2 in clarinet synthesis algorithms. While

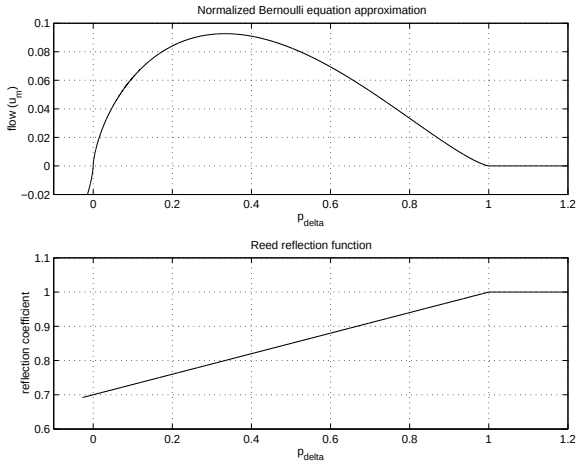

Figure 2: Bernoulli static flow expression (top); Simplified reed reflection function (bottom).

the behavior of the reed function plays an important role in the overall quality of a synthesis model, the memory-less system is adequate for the purposes of evaluating the various air column models explored here.

3 The Conical Waveguide

Wave propagation along the principal axis of a duct of uniform cross-section can be solved in terms of one-dimensional traveling *plane* waves with *real* wave impedance. Propagation along the principal axis of a conic frustum can be solved in terms of one-dimensional traveling *spherical* waves with *complex, location-dependent* wave impedance. In general, expressions describing the interaction of spherical waves will be frequency-dependent, while those for plane-wave scattering are often simple scalar functions.

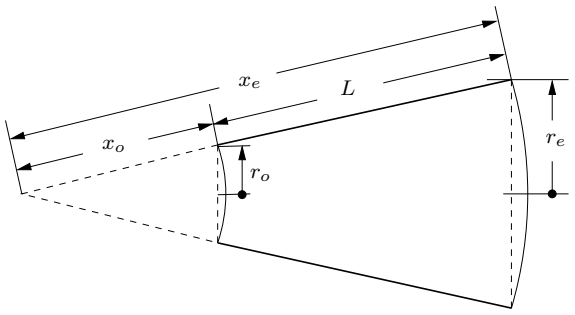

Figure 3: A conical waveguide.

3.1 The Equivalent Circuit

The acoustic properties of a conic frustum can be represented by an equivalent circuit consisting of a uniform transmission line, two acoustic inertances, and a transformer, as shown in Fig. 4 [Benade 1988]. This representation suggests that a conical air column model can be implemented using a cylindrical waveguide, a scalar "turns ratio" multiplier, and appropriately designed inertance components at each end of the waveguide.

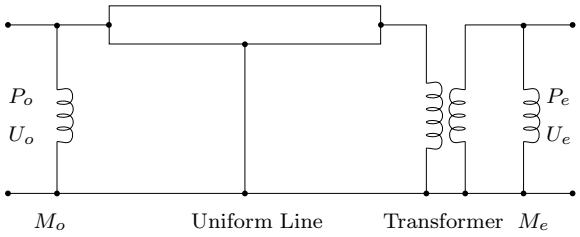

Figure 4: Equivalent circuit of a conical waveguide.

An ideal open end, represented by a load impedance of zero, will "short-circuit" an input/output inertance. The equivalent circuit for an open-open conic frustum then reduces to a uniform transmission line and a scalar transformer term. This confirms the fact that a cylindrical pipe open at both ends and an open-open conic section, each of length L, have equivalent longitudinal mode frequencies given by $f_n = nc/2L$, $n = 1, 2, 3, \ldots$, where c is the speed of wave propagation within the structures.

A pressure-controlled wind instrument excitation mechanism, such as a saxophone reed-mouthpiece or trumpet player lip-reed, functions as a nearly rigid, time-varying termination at an air column input. When attached to the input of a conical waveguide, the parallel driver impedance and input inertance (M_o) combination plays a significant role in determining the overall behavior of the air column.

3.2 Properties of Conic Frusta

It is generally agreed that harmonically aligned air column mode ratios better support a stable "regime of oscillation" via mode cooperation [Worman 1971]. It is thus expected that a synthesis model incorporating a nonlinear excitation mechanism will likewise benefit from such mode cooperation in attempting to produce a robust, stable oscillatory regime.

Ayers et al. [1985] presents an exploration of the properties of conic frusta. Of particular note, the mode ratios for truncated closed-open frusta of length L are shown to vary with respect to the parameter β as depicted in Fig. 5. β can be defined in terms of the ratio of input to output end radii, r_o/r_e, or in terms of the ratio $x_o/(x_o + L)$, where x_o is the length of the missing, truncated apical section (see Fig. 3). A complete cone is given by $\beta = 0$, while a closed-open cylinder is given by

$\beta = 1$. It should be obvious from Fig. 5 that any closed-open truncated conical section will have inharmonic mode ratios and that the extent of this inharmonicity is dependent on the dimensions of the frustum. Attempts at robust synthesis using a model which correctly simulates the behavior of a truncated conical section may in turn be hindered.

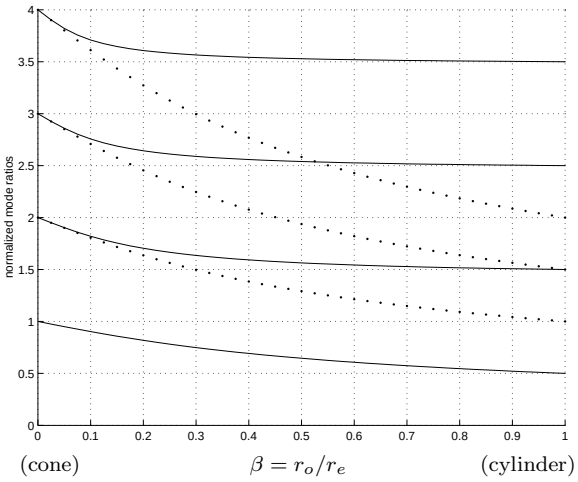

Figure 5: Modal frequencies for a closed-open conic frustum normalized by the fundamental frequency of an open pipe of the same length as the frustum. The dotted curves indicate integer relationships to the first mode.

Benade [1976] reports that the effects of truncation can be reduced by utilizing a reed/mouthpiece cavity with an equivalent volume equal to that of the missing conical section. This constraint is based on a lumped characterization of the reed/mouthpiece cavity, which is only appropriate for low-frequency modes whose wavelengths are large in comparison to the dimensions of the cavity. Higher-frequency modes are less likely to benefit from such a change because they are more directly affected by changes in waveguide shape.

Figure 6 plots the mode ratios for a cylinder-cone compound horn designed so that the cylindrical section volume is equal to the truncated conic section volume. For $\beta = 1$, the structure is of infinite length and all its modes converge to zero. In comparison with Fig. 5, the compound horn displays nearly harmonic mode ratios out to values of β in the range 0.2–0.3.

Another property of conic frusta can be directly attributed to the input inertance element, M_o, in the equivalent circuit (Fig. 4). The inertance, whose magnitude varies with the parameter β, tends to "shunt" low-frequency wave components, thus imposing a "high-pass" characteristic on the resulting air column mode structure. For longer conic sections, the lowest modes can be significantly attenuated, which in turn destabilizes oscillatory regimes dependent on these modes. This

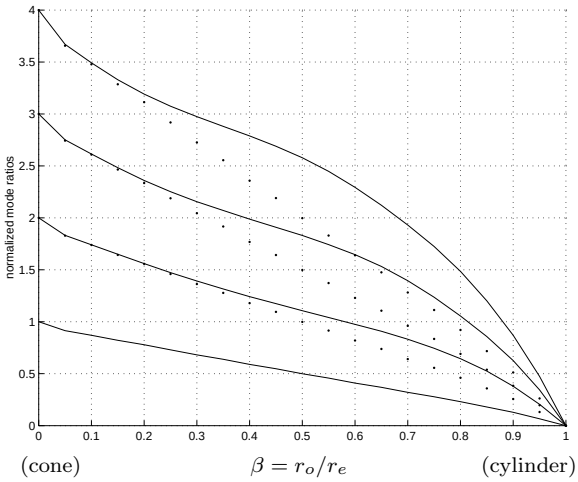

Figure 6: Modal frequencies for a closed-open, cylinder-cone compound horn in which the cylindrical section volume is equivalent to the missing conic section volume. The dotted curves indicate integer relationships to the first mode.

behavior is often apparent in the lowest notes of saxophones, which tend to be difficult to control under soft playing conditions. Figure 7 shows an example conic section input impedance in which this effect is demonstrated. The smooth curve indicates the combined influence of the conicity inertance and the open-end load impedance.

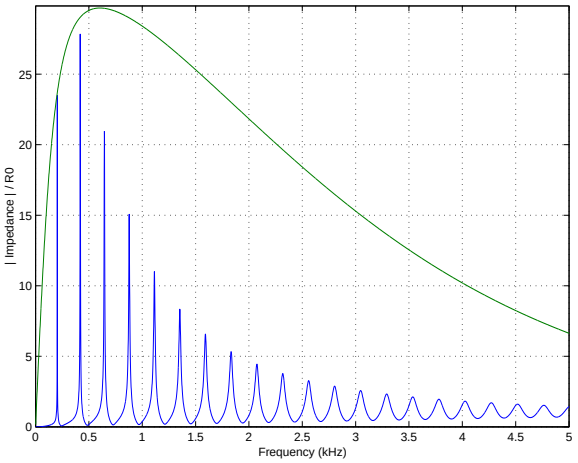

Figure 7: An example conic frustum input impedance.

4 Model Approaches

In order to implement the equivalent circuit of a conical waveguide using digital waveguide techniques, it is necessary to express the lumped impedance elements of Fig. 4 in terms of traveling-wave parameters and then convert these expressions to discrete-time filters. The impedance of the input inertance, given in terms of a Laplace

transform, is $M_o(s) = (\rho x_o/A_o)\, s$, where ρ is the mass density of air, A_o is the area of the spherical wavefront at the waveguide input, and s is Laplace transform frequency variable. The effective impedance at the waveguide input is determined as the parallel combination of M_o and an input load impedance. If the input is rigidly terminated, the input load is infinite and the pressure-wave reflectance is given by:

$$\mathcal{R}_o(s) \triangleq \frac{P_o^-(s)}{P_o^+(s)} = \frac{M_o(s) - Z_o}{M_o(s) + Z_o} = \frac{x_o s - c}{x_o s + c},$$

where $Z_o = \rho c/A_o$ is a real, locally defined characteristic impedance parameter. The reflectance filter, discretized with the bilinear transform, is

$$\mathcal{R}_o(z) = \frac{-a_1 - z^{-1}}{1 + a_1 z^{-1}}, \quad \text{where} \quad a_1 = \frac{c - \alpha x_o}{c + \alpha x_o},$$

and α is the bilinear transform constant which controls frequency warping. This first-order allpass filter accurately accounts for the phase delay experienced by pressure traveling-wave components reflecting from a rigid input termination in a conical waveguide. The output inertance, M_e, tends to be less significant than that at the input, particularly in the presence of an open-end load impedance. In general, a single output reflectance filter can be designed based on the parallel combination of M_e and an appropriate open-end impedance characterization.

Figure 8 shows a truncated conic structure and the corresponding digital waveguide block diagram, using input and output reflectance filters as discussed above.

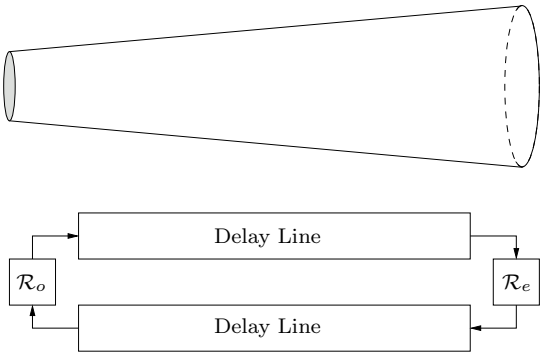

Figure 8: A closed-open conic structure (top) and its digital waveguide block diagram (bottom).

The goal here is to model a conical bore instrument system by attaching a simple, memoryless, non-linear excitation mechanism to a conical air column representation. The traditional reed function/air column coupling, however, is derived for an input cylindrical section using a real wave impedance. It is not a simple process to rederive the reed function using the complex wave impedance of a conic frustum. Even if we ignored this complication, direct coupling of the reed function to the allpass inertance element at the input to the conical "circuit" would produce a delay-free loop in the digital waveguide implementation. These constraints lead to the modeling approach discussed first in this section.

All of the models to be presented have been implemented using the Synthesis ToolKit in C++ (STK) [Cook and Scavone 1999], allowing control and exploration with the model parameters in realtime.

4.1 The "Cyclone"

The "cyclone" conical bore model is based on a compound cylindrical-conical segment air column model as illustrated at the top of Fig. 9. The input cylindrical section roughly models the instrument mouthpiece cavity and its use avoids the complications previously discussed with respect to the nonlinear driver. In addition, the cylindrical section can be designed to have an equivalent volume equal to the missing conic section volume. Assuming no diameter discontinuity at the cylinder-cone junction, this constraint is met using a cylindrical section length equal to $x_o/3$. It should be noted that Benade distinguishes between a cavity's physical and equivalent volumes under playing conditions, which are typically not the same. For the simplified reed function used in this implementation, however, it is reasonable to ignore this difference.

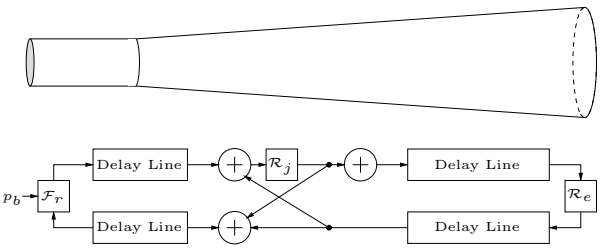

Figure 9: "Cyclone" physical structure (top) and digital waveguide block diagram (bottom).

The cylinder-cone junction filter is derived assuming continuity of pressure and conservation of volume velocity and then discretized using the bilinear transform as:

$$\mathcal{R}_j^-(z) = \mathcal{R}_j^+(z) = -\frac{\gamma}{\alpha + \gamma}\left(\frac{1 + z^{-1}}{1 - a_1 z^{-1}}\right),$$

where α is the bilinear transform constant,

$$\gamma = \frac{c}{2x_o}, \qquad a_1 = \frac{\alpha - \gamma}{\alpha + \gamma},$$

c is the speed of wave propagation in the structure, and x_0 is the length of the truncated conic

section. This expression could just as well have been derived from the parallel combination of the input inertance M_o and the wave impedance of the input cylindrical section.

The junction transmittance magnitude response ($|1 + \mathcal{R}|$) is shown in Fig. 10 for various values of x_o. The "high-pass" filter characteristic associated with the conical waveguide input inertance term can vary significantly depending on the frustum dimensions. Shorter values of x_o correspond to steeper flare rates, which produce greater wave discontinuity at the junction and greater low-frequency attenuation. While this might appear to imply a preference for less steeply flared conic sections, it should be remembered that larger values of x_0 correspond to larger values of β in Fig. 5 and thus greater mode inharmonicity. The result is a design conflict between junction discontinuity, which destabilizes the lower air column modes, and mode harmonicity.

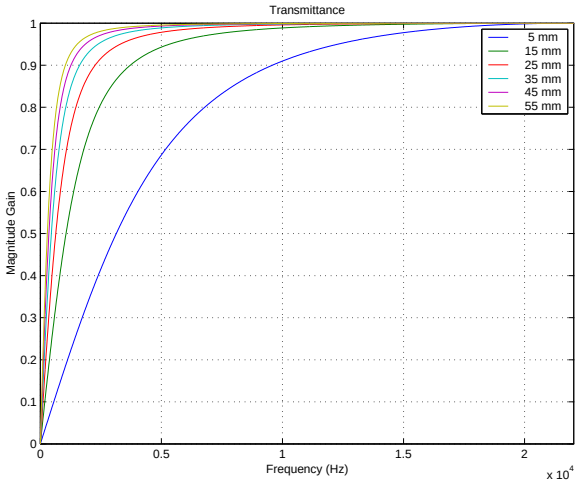

Figure 10: The cylinder-cone junction transmittance for various values of truncation x_o.

The cylinder-cone junction can be implemented using a single first-order digital filter, as discussed by Smith [1991], Välimäki and Karjalainen [1994] and others. A block diagram of the resulting digital waveguide model is shown in Fig. 9.

Figure 11 displays the input impedance and sound spectrum produced by an example "cyclone" waveguide model. Despite significant inharmonicity of the input impedance peaks, the resulting synthesis spectrum is harmonic and exhibits contributions from "misaligned" peaks as a result of the non-linear regenerative process.

The sounds produced by the "cyclone" model have a distinctive saxophone quality, though the instabilities associated with truncated conic frusta as outlined in earlier sections are present and the functional parameter space can be difficult to assess.

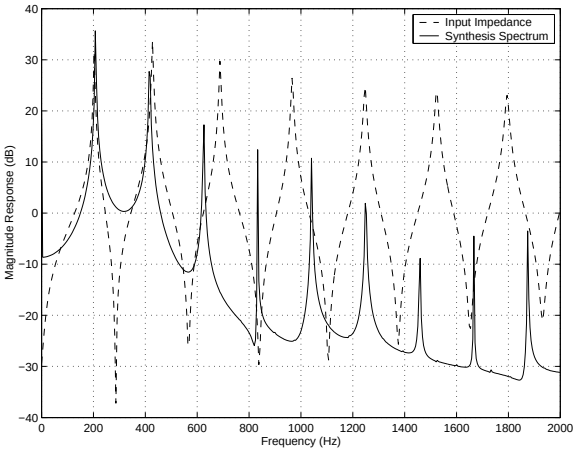

Figure 11: Example "cyclone" model input impedance and synthesized sound spectrum.

4.2 The Cylindrical Saxophone

With the help of Fig. 4, we can develop an alternative interpretation of the "cyclone" model as two uniform transmission-line elements separated by a shunt inertance component. If the inertance is implemented as a small, mass-like "register hole", we have the physical structure shown in Fig. 12 and a model which is equivalent to Benade's "cylindrical saxophone" [Benade 1988].

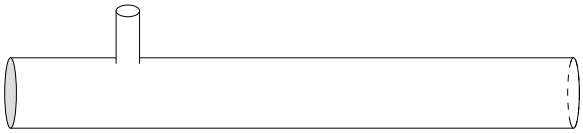

Figure 12: The "cylindrical saxophone" model.

The impedance of an open-hole shunt inertance, given in terms of a Laplace transform, is:

$$Z(s) = \frac{\rho t}{A_h} s,$$

where t is the effective height of the hole and A_h is its cross-sectional area.

The junction filter derived for the register hole is [Scavone and Cook 1998]

$$\mathcal{R}_j^-(z) = \mathcal{R}_j^+(z) = -\frac{\gamma}{\alpha + \gamma}\left(\frac{1 + z^{-1}}{1 - a_1 z^{-1}}\right),$$

where α is the bilinear transform constant,

$$\gamma = \frac{cA_h}{2tA_o}, \qquad a_1 = \frac{\alpha - \gamma}{\alpha + \gamma},$$

and A_o is the cross-sectional area of the cylindrical pipe.

The "cyclone" and "cylindrical" circuits are equivalent with parameters related by:

$$x_o = \frac{A_o t}{A_h} \quad \text{or} \quad t = \frac{x_o A_h}{A_o}.$$

It is interesting to compare the corresponding conic frustum and register hole parameters. We see that the length of the truncated conic section is proportional to register hole height and inversely proportional to register hole radius.

The "cylindrical" model parametrization scheme has the added benefit of allowing synthesis of either a clarinet or a saxophone-like system via control of the filter gain parameter γ. The register hole is effectively closed when its radius is zero, which results in $\gamma = 0$ and $\mathcal{R}_j(z) = 0 \; \forall \; z$. Since there is no junction discontinuity, the system reduces to a single continuous cylindrical section. The "cylindrical saxophone" model presents a slightly more complex parameter space (parameters t and A_h versus x_o), though its response is similar to the "cyclone" model.

4.3 The Virtual "Blowed String"

The "cyclone" and "cylindrical saxophone" models offer acoustically accurate representations of their corresponding physical manifestations. In addition, they inherit the various potential disadvantages previously discussed for these structures, including modal inharmonicity and weak low frequency mode support. An accurate physical model does not always make the best musical instrument.

It is an interesting exercise to throw physical reality aside and to consider a more abstract approach to the design of an acoustic air column or resonator. In order to synthesize conical bore instrument sounds using a pressure-controlled driving mechanism, we desire a stable structure with the following features:

- resonance frequencies given by $nc/2L$, for $n = 1, 2, 3, \ldots$
- an input point with sufficient pressure fluctuation to drive a reed function.

An open-open cylinder possesses the desired modal characteristic. However, air pressure variations are constrained to zero at an open pipe end, or pressure node.

Another system possessing the desired resonance structure is a stretched string, fixed at both its ends. The string and open pipe share a variety of analogous properties via an exchange of mechanical and acoustic variables. Likewise, there are similarities in the way that each system can be driven. A string can be bowed, plucked, or struck at any point along its length except near either of its ends, where the mechanical velocity is constrained to zero. By analogy, it should be possible to drive an open pipe by applying a pressure-controlled excitation at any point along its length other than near an open end. This possibility has not been realized because no appropriate pressure-controlled device has been developed which can be positioned inside a pipe without modifying its acoustic properties.

Digital synthesis systems, however, are not limited by the physical constraints of reality. Inspired by the bowed string, the "blowed string" model incorporates an open-open cylindrical air column structure and a non-linear reed function, applied at a "blowing" point which can be varied along the length of the pipe. The "blowed string" digital waveguide block diagram is shown in Fig. 13. One end of the pipe is modeled with a lossy reflectance filter $\mathcal{R}_e$, while the other end is represented by an ideal impedance of zero (which corresponds to the pressure wave multiplier -1). The internal pressure at any point within the air column is calculated by summing the two traveling-wave components. The reed function uses the internal pressure value, together with the current "blowing" pressure, to determine an appropriate function output.

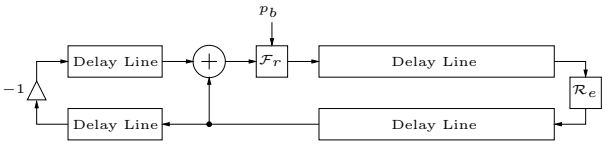

Figure 13: "Blowed string" block diagram.

The actual "blowed string" implementation can be simplified with respect to the block diagram of Fig. 13. In practice, each delay-line pair can be combined into a single unit and the scalar multiplier can be commuted to a more convenient implementation point. Thus, the entire system can be implemented using two interpolating delay lines, a simple first-order lowpass filter, an adder, and a non-linear reed reflection function. It is even possible to use just a single delay line with a fractional-delay tap output.

Variation of the blow point can provide a wide range of timbres. The relationship between bow position and harmonic content of a bowed-string sound applies to this structure as well. When "blowed" at $1/n$th the distance from a pipe end, modes at integer multiples of n are not excited. By positioning the "blow point" at the center of the air column, the characteristic timbre of a clarinet is achieved. In addition to being the most computationally efficient model discussed, the "blowed string" displays exceptionally robust behavior over a wide parameter space.

Figure 14 displays the input impedance and sound spectrum produced by the "blowed string" waveguide model with a "blow" point positioned at 1/5 the distance from an open end. The attenuation of the 5th harmonic is clearly evident. In gen-

eral, there is significantly more harmonic content in this sound than was present in the previously discussed models.

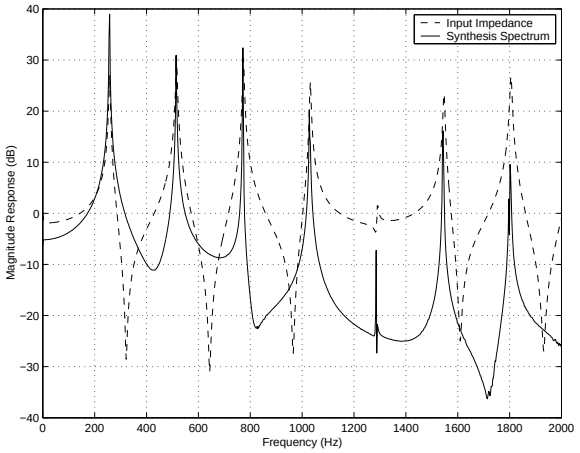

Figure 14: Example "blowed string" model input impedance and synthesized sound spectrum.

5 Summary

The "cyclone" and "cylindrical saxophone" approaches to conical bore modeling provide acoustically accurate representations of their respective physical systems. For the purposes of acoustic study and further explorations regarding the properties of conic frusta, these models offer efficient structures for discrete-time implementation. In addition, the two equivalent parameterization schemes provide an interesting duality and perspective on the acoustic behavior of conical waveguides. With respect to synthesis, these models produce good sonic results within a somewhat complex parameter space.

The virtual "blowed string", though potentially less appealing to acoustic purists, provides a robust and flexible synthesis model capable of generating a wide range of possible timbres, including both cylindrical and conical bore sounds. This model suggests an interesting analogy to the bowed string based on an abstract or "physically informed" view of air column acoustics.

References

D. R. Ayers, L. J. Eliason, and D. Mahgerefteh. The conical bore in musical acoustics. *Am. J. Phys.*, 53(6):528–537, June 1985.

A. H. Benade. *Fundamentals of Musical Acoustics*. Oxford University Press, New York, 1976.

A. H. Benade. Equivalent circuits for conical waveguides. *J. Acoust. Soc. Am.*, 83(5):1764–1769, May 1988.

P. R. Cook. A meta-wind-instrument physical model, and a meta-controller for real time performance control. In *Proc. 1992 Int. Computer Music Conf.*, pages 273–276, San Jose, California, 1992. Comp. Music Assoc.

P. R. Cook and G. P. Scavone. Synthesis ToolKit in C++, Version 2.02. In *SIGGRAPH 1999, Course Notes #23, Virtual Worlds/Real Sounds*. Association for Computing Machinery, 1999.

G. P. Scavone and P. R. Cook. Real-time computer modeling of woodwind instruments. In *Proc. Int. Symp. on Musical Acoustics (ISMA-98), Leavenworth, WA*, pages 197–202, June 1998.

J. O. Smith. Efficient simulation of the reed-bore and bow-string mechanisms. In *Proc. 1986 Int. Computer Music Conf.*, pages 275–280, The Hague, Netherlands, 1986. Comp. Music Assoc.

J. O. Smith. Waveguide simulation of non-cylindrical acoustic tubes. In *Proc. 1991 Int. Computer Music Conf.*, pages 304–307, Montreal, Canada, 1991. Comp. Music Assoc.

J. O. Smith. Physical modeling using digital waveguides. *Computer Music J.*, 16(4):74–91, Winter 1992. Special issue: Physical Modeling of Musical Instruments, Part I.

V. Välimäki and M. Karjalainen. Digital waveguide modeling of wind instrument bores constructed of truncated cones. In *Proc. 1994 Int. Computer Music Conf.*, pages 423–430, Århus, Denmark, 1994. Comp. Music Assoc.

M. P. Verge. *Aeroacoustics of Confined Jets, with Applications to the Physical Modeling of Recorder-Like Instruments*. PhD thesis, Eindhoven University of Technology, 1995.

C. Vergez and X. Rodet. Experiments with an artificial mouth for trumpet. In *Proc. Int. Symp. on Musical Acoustics (ISMA-98), Leavenworth, WA*, pages 153–158, June 1998.

W. E. Worman. *Self-Sustained Nonlinear Oscillations of Medium Amplitude in Clarinet-Like Systems*. PhD thesis, Case Western Reserve University, 1971.